JOC Article
pubs.acs.org/joc

Dissecting a Dyotropic Rearrangement

Rebecca L. Davis and Dean J. Tantillo*

Department of Chemistry University of California, Davis, One Shields Avenue, Davis, California 95616

tantillo@chem.ucdavis.edu

Received December 18, 2009

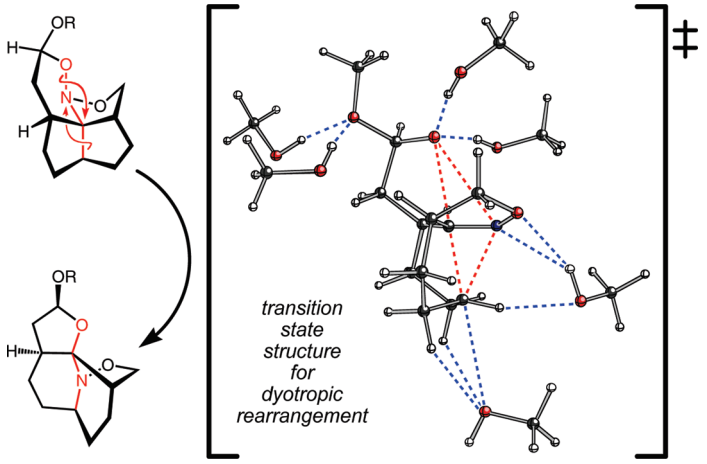

Herein we describe density functional theory calculations on nitroso acetal-to-aminal rearrangements reported by Denmark and co-workers. Our calculations indicate that various structural (ring strain, hyperconjugation, anomeric effects) and environmental (both specific and nonspecific solvation) factors greatly influence the ease of rearrangement. Our calculations also indicate that both concerted and stepwise mechanisms are energetically viable.

Introduction

Despite their potential application in constructing complex polycycles, dyotropic rearrangements, in which "two σ-bonds simultaneously migrate intramolecularly",[1] have been used somewhat infrequently in synthesis.[1−3] This, perhaps, is a result of difficulties in predicting and controlling the occurrence of such reactions. In fact, some of the most useful dyotropic rearrangements have been encountered unexpectedly. Take, for example, the rearrangement shown in Scheme 1, which was discovered by Denmark and co-workers while trying to synthesize an azafenestrane.[3] The expected product (**3**; Scheme 2) of a [4 + 2]/(3 + 2) double cycloaddition cascade was not observed, and instead,

SCHEME 1

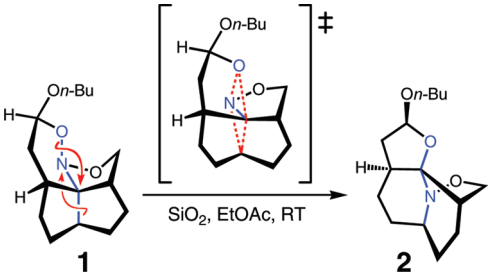

(1) (a) Reetz, M. T. *Angew. Chem., Int. Ed. Engl.* **1972**, *11*, 129–130. (b) Reetz, M. T. *Angew. Chem., Int. Ed. Engl.* **1972**, *11*, 130–131. (c) Reetz, M. T. *Tetrahedron* **1973**, *29*, 2189–2194. (d) Reetz, M. T. *Adv. Organomet. Chem.* **1977**, *16*, 33–65. (e) Hoffmann, R.; Williams, J. E., Jr. *Helv. Chim. Acta* **1972**, *55*, 67–75. These papers emphasize the connections between dyotropic reactions and related pericyclic processes. (f) The reaction discussed herein is an example of a "type I" dyotropic rearrangement, in which two groups migrate in different directions such that their positions are interchanged.[1a]

(2) Representative examples: (a) Zhang, X.; Houk, K. N.; Lin, S.; Danishefsky, S. J. *J. Am. Chem. Soc.* **2003**, *125*, 5111–5114. (b) Li, W.; LaCour, T. G.; Fuchs, P. L. *J. Am. Chem. Soc.* **2002**, *124*, 4548–4549. (c) Singh, G.; Linden, A.; Abou-Hadeed, K; Hansen, H.-J. *Helv. Chim. Acta* **2002**, *85*, 27–59. (d) Mulzer, J.; Hoyer, K.; Müller-Fahrnow, A. *Angew. Chem., Int. Ed. Engl.* **1997**, *36*, 1476–1478. (e) Lemos, E.; Porée, F.-H.; Commerçon, A.; Betzer, J.-F.; Pancrazi, A.; Ardisson, J. *Angew. Chem., Int. Ed.* **2007**, *46*, 1917–1921. (f) Purohit, V. C.; Matla, A. S.; Romo, D. *J. Am. Chem. Soc.* **2008**, *130*, 10478–10479. (g) Elpert, M.; Maichle-Mössmer, C.; Maier, M. E. *J. Org. Chem.* **2002**, *67*, 8692–8695. (h) A recent comprehensive review: Fernández, I.; Cossío, F. P.; Sierra, M. A. *Chem. Rev.* **2009**, *109*, 6687–6711.

(3) (a) Denmark, S. E.; Montgomery, J. I. *Angew. Chem., Int. Ed.* **2005**, *44*, 3732–3736. (b) Denmark, S. E.; Montgomery, J. I.; Kramps, L. A. *J. Am. Chem. Soc.* **2006**, *128*, 11620–11630.

DOI: 10.1021/jo902685x Published on Web 02/01/2010

SCHEME 2

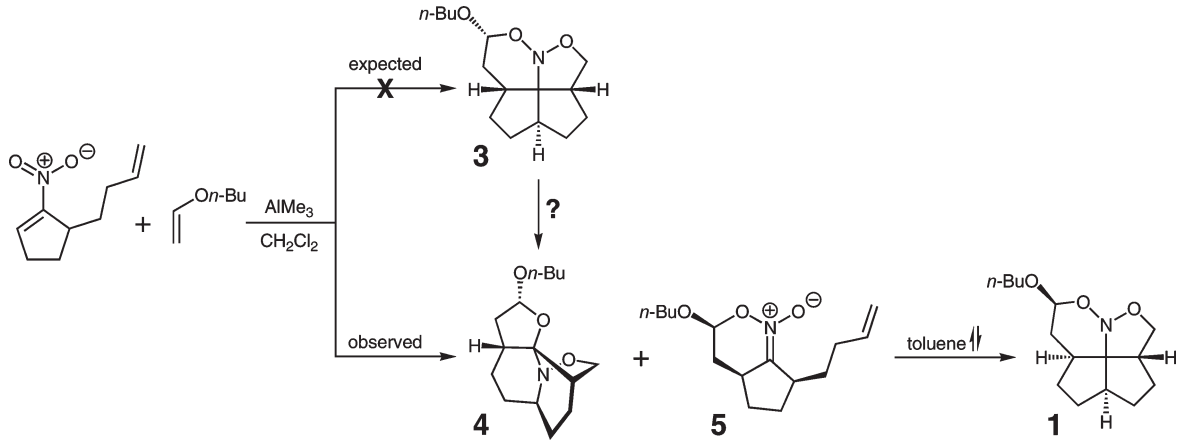

products **4** and **5** were isolated.[3] It was proposed that the desired compound had actually formed but then undergone a dyotropic rearrangement (**3** → **4**). Compound **5**, the product of only a single cycloaddition, was heated to induce a second cycloaddition, and although nitroso acetal **1** was formed, it was found to rearrange to aminal **2** upon exposure to SiO_2 and ethyl acetate (Scheme 1). Clearly, dyotropic rearrangements are facile for structures like **1** and **3**, but why this is so and the mechanisms of these rearrangements are not entirely clear. Herein we describe the results of quantum chemical calculations aimed at characterizing the mechanisms of these rearrangements and quantifying the contributions of various structural and environmental factors to their barriers.

Methods

All calculations were run using GAUSSIAN03.[4] Geometries were optimized without symmetry constraints at the B3LYP/6-31G(d) level of theory.[5] All structures were characterized by frequency analysis and reported energies from B3LYP/6-31G(d) calculations include zero-point energy (ZPE) corrections scaled by 0.9806.[6] Intrinsic reaction coordinate (IRC) calculations were also used to characterize transition-state structures (see the Supporting Information for details).[7] Free energies were calculated at room temperature. All reported barriers are based on the productive conformer of the reactant. Selected structures were also optimized using B3LYP/6-31+G(d,p) (see the Supporting Information for details). Solvent calculations using water (ε = 78.39) or methanol (ε = 32.63) were run using the CPCM method with UAKS radii.[8] Structural images were created using *Ball & Stick*.[9]

Results and Discussion

The 1-to-2 Rearrangement. Our study began with an examination of the **1**-to-**2** dyotropic rearrangement

SCHEME 3

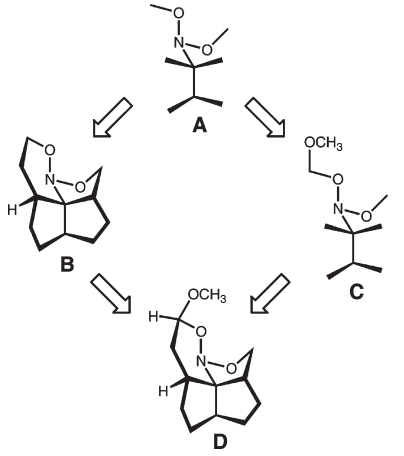

(Scheme 1). Several simplified models of nitroso acetal **1** were utilized so that we could pinpoint the contributions of specific structural features to the rearrangement barrier (Scheme 3). The simplest of these, **A**, contains the rearranging O−N−C−C substructure (blue in Scheme 1) and methyl substituents on each of these atoms that bear alkyl groups in **1**. This model is useful in assessing the inherent reactivity of the nitroso acetal core of **1**. A transition-state structure for the concerted (and quite synchronous) dyotropic rearrangement of **A** was located (Figure 1). The barrier for rearrangement of **A** through this transition-state structure was computed to be nearly 70 kcal/mol (Figure 1). Clearly, this barrier is much too high to correspond to facile rearrangement at room temperature, as observed for **1**, so structural features present in **1** or features of the reaction environment must contribute significantly to lowering this barrier.

Our second model system, **B** (Scheme 3), includes the polycyclic ring system present in **1**. Dyotropic rearrangement of **B** (again, a concerted process) is predicted to have a barrier of just over 50 kcal/mol (Figure 2), indicating that the geometric constraints imposed by the polycyclic ring system lower the barrier by approximately 15−20 kcal/mol (compare Figures 1 and 2). This is most likely a result of reactant destabilization, i.e., preorganizing the reactant into a strained but reactive geometry. Note that the length of the

(4) *GAUSSIAN03*, revision B.04. Frisch, M. J. et al., Gaussian, Inc., Pittsburgh, PA, 2003; the full reference can be found in the Supporting Information.

(5) (a) Becke, A. D. *J. Chem. Phys.* **1993**, *98*, 5648–5652. (b) Becke, A. D. *J. Chem. Phys.* **1993**, *98*, 1372–1377. (c) Lee, C.; Yang, W.; Parr, R. G. *Phys. Rev. B* **1988**, *37*, 785–789. (d) Stephens, P. J.; Devlin, F. J.; Chabalowski, C. F.; Frisch, M. J. *J. Phys. Chem.* **1994**, *98*, 11623–11627.

(6) Scott, A. P.; Radom, L. *J. Phys. Chem.* **1996**, *100*, 16502–16513.

(7) (a) Gonzalez, C.; Schlegel, H. B. *J. Phys. Chem.* **1990**, *94*, 5523–5527. (b) Fukui, K. *Acc. Chem. Res.* **1981**, *14*, 363–368.

(8) (a) Barone, V.; Cossi, M. J. *J. Phys. Chem. A* **1998**, *102*, 1995–2001. (b) Barone, V.; Cossi, M.; Tomasi, J. *J. Comput. Chem.* **1998**, *19*, 404–417. (c) Takano, Y.; Houk, K. N. *J. Chem. Theor. Comput.* **2005**, *1*, 70–77.

(9) Müller, N.; Falk, A. *Ball & Stick V.3.7.6*; molecular graphics application for MacOS computers; Johannes Kepler University: Linz, 2000.

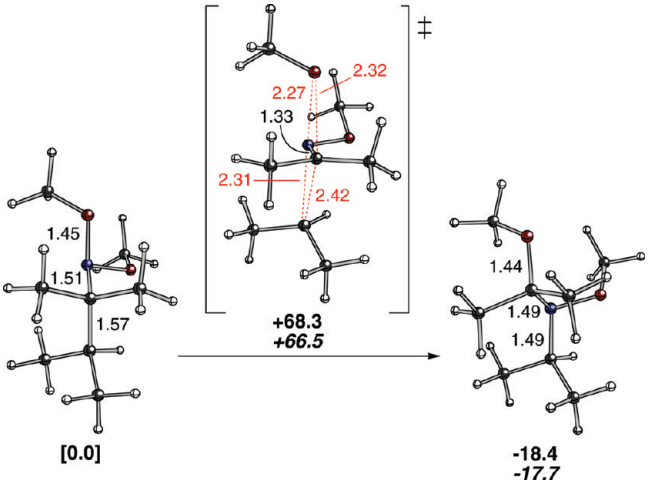

FIGURE 1. B3LYP/6-31G(d)-optimized geometries of reactant, transition-state structure, and product for the rearrangement of **A**. All energies are reported in kcal/mol and are relative to the energy of the reactant (ZPE-corrected energies in normal text; free energies at room temperature in italics). Selected bond lengths are given in Å.

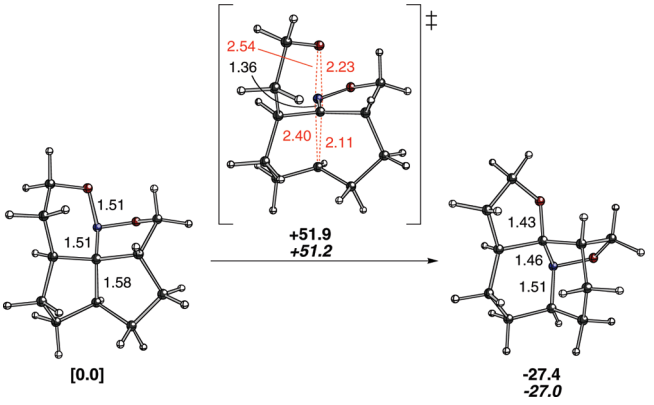

FIGURE 2. B3LYP/6-31G(d)-optimized geometries of reactant, transition-state structure, and product for the rearrangement of **B**. All energies are reported in kcal/mol and are relative to the energy of the reactant (ZPE-corrected energies in normal text; free energies at room temperature in italics). Selected bond lengths are given in Å.

N−O bond in the reactant that will break during the rearrangement is significantly longer in **B** than in **A** (compare Figures 1 and 2). Note also that both migrating groups are closer to the carbon atom of the C−N unit across which they travel in the transition-state structure for rearrangement of **B**.

Our third model system, **C** (Scheme 3), lacks the polycyclic ring system but contains the acetal substructure present in **1** (a methyl group was used in place of the butyl group in **1** for simplicity). The computed barrier for concerted dyotropic rearrangement of **C** (through the transition-state structure shown in Figure 3) is approximately 60 kcal/mol, indicating that the acetal group contributes approximately 7 kcal/mol toward lowering the rearrangement barrier (compare Figures 1 and 3). This effect has at least two possible origins. First, it could be inductive in nature. The electronegative oxygen of the methoxy group will withdraw electron density from the migrating oxygen, thereby delocalizing the negative charge that is accumulating at this position as

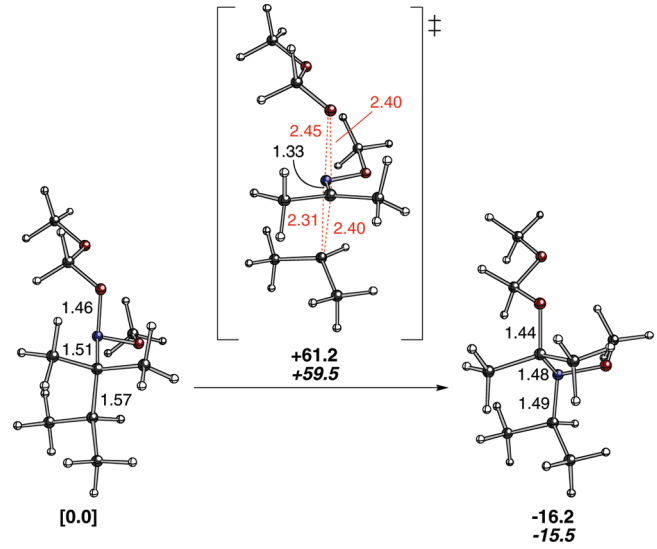

FIGURE 3. B3LYP/6-31G(d)-optimized geometries of reactant, transition-state structure, and product for the rearrangement of **C**. All energies are reported in kcal/mol and are relative to the energy of the reactant (ZPE-corrected energies in normal text; free energies at room temperature in italics). Selected bond lengths are given in Å.

the transition-state structure is reached (this charge build-up can be seen in the electrostatic potential surfaces shown in Figure 4 for representative reactants and transition-state structures). Second, it could be the result of an orbital interaction in which a lone pair on the migrating oxygen donates electron density into the antibonding orbital of the C−OCH_3 bond (an anomeric effect), again withdrawing electron density from the migrating oxygen. It is likely that both of these effects contribute. Note that both partial bonds to the migrating oxygen are longer in the transition-state structure for model **C** than in the transition-state structure for model **A** (compare Figures 1 and 3).

If the effects of the polycyclic framework and acetal are additive, then we would predict that a system containing both of these elements would have a barrier of approximately 45 kcal/mol. Our calculations on such a system, model system **D** (Scheme 3 and Figure 5), predict a barrier for rearrangement of just over 45 kcal/mol. Note that in this system (compare with **B**; Figure 2), the boat conformation of the reactant allows for a favorable anomeric interaction between a lone pair of the endocyclic oxygen and the σ^* orbital of the C−O bond to the methoxy group. In the resulting transition-state structure, this effect would be mitigated to some extent by donation of a lone pair on the methoxy group into the antibonding $\sigma^*_{C-O(migrating)}$ orbital. Even so, the effects highlighted by models **B** and **C** appear to be approximately additive. The barrier predicted for **D** (which differs from **1** only by the substitution of a methyl group for a butyl group) is still not low enough to correspond to the experimentally observed reactivity, however. This leads us to believe that the environment in which the dyotropic rearrangement occurs is also making a large contribution toward its facility.

This contention was addressed through two types of calculations: those involving explicit solvent molecules and those involving immersion in a solvent continuum. To explore the

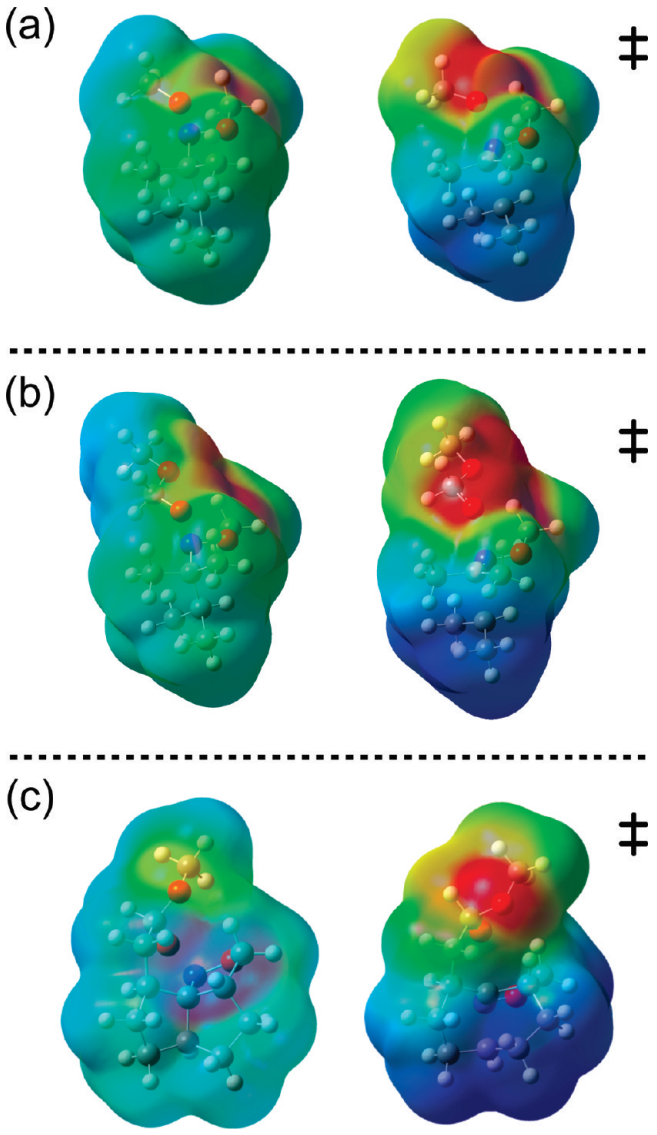

FIGURE 4. Electrostatic potential (ESP) maps of reactants and transition-state structures for models (a) **A**, (b) **C**, and (c) **D**. ESP maps were constructed using an isovalue of 0.0004 with a charge range of −0.045 to 0.030.

effects of the latter, rearrangement of **D** (Scheme 3) was reexamined in the presence of methanol or water (representative polar environments) using calculations in which the solvent was treated as a homogeneous field (see the Methods section for details). Note that the dipole moment computed for the transition-state structure for rearrangement of **D** is 4 D greater than that for the reactant (see also Figure 4c),[10] suggesting that the transition-state structure should be selectively stabilized in polar environments. In methanol or water, the rearrangement barrier was computed to be 36−38 kcal/mol (based on fully reoptimized structures; see the Supporting Information for details), indicating that nonspecific solvation can lower the rearrangement barrier by up to 12 kcal/mol. Note also that the C−O and N−O distances in the transition-state structure that was fully optimized in a methanol continuum are longer than those in the gas phase (2.54 and 2.92 Å, respectively; compare with Figure 5), consistent with the polar environment promoting charge separation.

To determine the effects of explicit interactions between solvent molecules (or specific sites in slightly acidic bulk silica) and transition-state structures, several model systems were designed in which methanol molecules interact with either a lone pair or hydrogen on the nitrosoacetal (**E**−**J**; Figure 6; see the Supporting Information for geometries).[12] Stabilizing the accumulation of negative charge on the migrating oxygen through hydrogen bonding (models **E** and **F**, which differ in terms of which lone pair of the migrating oxygen participates in hydrogen bonding) reduces the barrier for dyotropic rearrangement by 6−9 kcal/mol (compare **E** and **F** to **D**). Hydrogen bonding to the oxygen of the methoxy substituent (model **G**) also stabilizes the negative charge build-up in the transition state structure by making the methoxy group a stronger σ-electron-withdrawing group (which would strengthen both the inductive and anomeric

(10) Computed partial charges (below; CHelpG[11] using B3LYP/-31G(d)) also reveal the build-up of negative charge on the migrating oxygen and an increase in positive charge on the migrating carbon as the transition-state structure is reached.

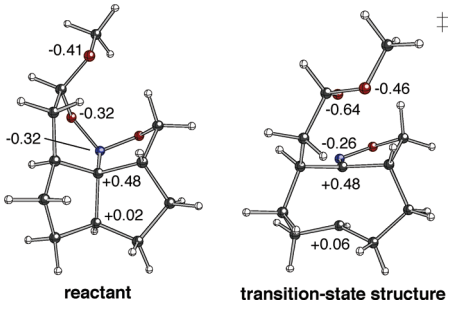

(11) Breneman, C. M.; Wiberg, K. B. *J. Comput. Chem.* **1990**, *11*, 361–373.

(12) An alternative pathway in which **D** undergoes nucleophilic attack by a methanol molecule at the migrating carbon was also explored. This pathway proved to be energetically unreasonable (see below). In addition, as the N−O bond is broken (along with C−C bond cleavage and C=N formation), the methoxy group rotates forward and the incipient O^- rotates away from the C=N substructure (presumably to release strain in the forming eight membered ring).

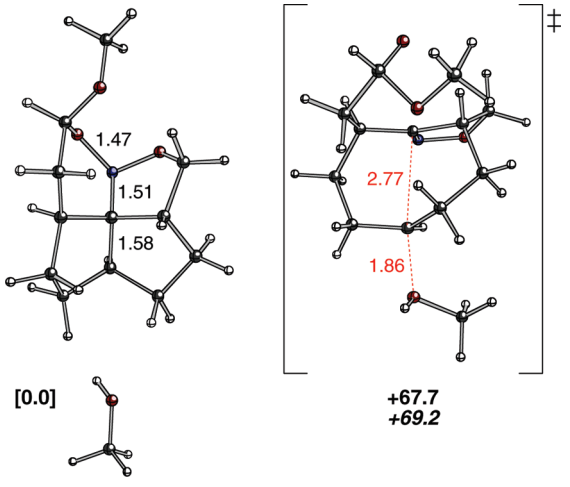

(13) We have observed similar effects for carbocations; see: (a) Hong, Y. J.; Tantillo, D. J. *J. Org. Chem.* **2007**, *72*, 8877–8881. (b) Lodewyk, M. J.; Gutta, P.; Tantillo, D. J. *J. Org. Chem.* **2008**, *73*, 6570–6579. (c) Hong, Y. J.; Tantillo, D. J. *J. Am. Chem. Soc.* **2009**, *131*, 7999–8015.

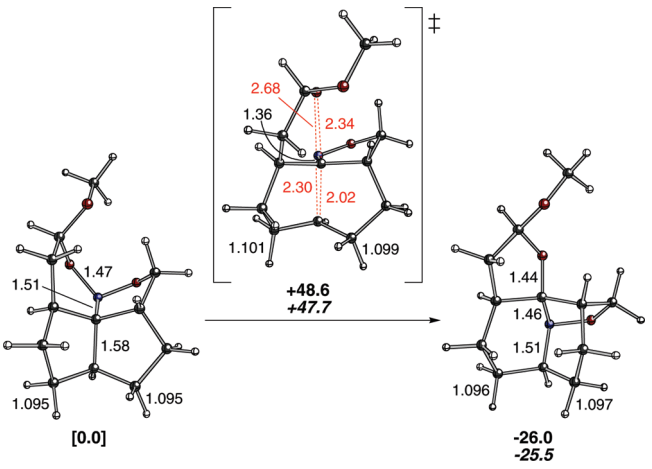

FIGURE 5. B3LYP/6-31G(d)-optimized geometries of reactant, transition-state structure, and product for the rearrangement of **D**. All energies are reported in kcal/mol and are relative to the energy of the reactant (ZPE-corrected energies in normal text; free energies at room temperature in italics). Selected bond lengths are given in Å.

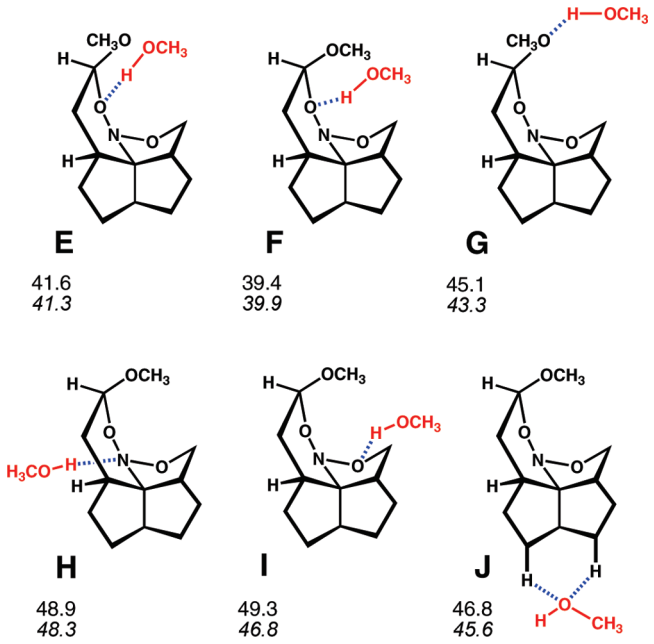

FIGURE 6. Computed barriers (B3LYP/6-31G(d); kcal/mol) for dyotropic rearrangements of models **E**−**J**. All energies are reported in kcal/mol and are relative to the energy of the starting material (ZPE-corrected energies in normal text; free energies at room temperature in italics).

effects described above), resulting in a reduction of the barrier of approximately 3−4 kcal/mol. Hydrogen bonding to the nitrogen (model **H**) or the oxygen in the 5-membered ring (model **I**) has only a small effect (< 1 kcal/mol) on the barrier. Model **J** reveals a particularly subtle effect. As the dyotropic rearrangement proceeds, the migrating carbon becomes somewhat electron deficient (see Figure 4c).[10] As a result, hyperconjugation between this center and the appropriately aligned adjacent C−H bonds intensifies, resulting in a slight increase in the C−H bond lengths (0.005 Å). The interaction of these C−H groups with the lone pairs of the solvent molecule strengthens this hyperconjugation, leading to a reduction of the barrier of approximately 2−3 kcal/mol.[13]

To examine the full extent to which explicit solvent interactions could lead to selective stabilization of the transition-state structure, several additional models containing multiple solvent molecules were designed (**K**−**O**, Figure 7; see the Supporting Information for geometries). When two solvent molecules hydrogen bond to the migrating oxygen (model **K**), the energy barrier is 4−7 kcal/mol less than the cases involving a single hydrogen bond (compare **K** to **E** and **F**). Note that one methanol molecule actually migrates to the oxygen of the five-membered ring during optimization of the reactant complex (analogous to complex **I**); although this is perhaps a computational artifact (in that the solute would be surrounded by solvent molecules in solution), it is consistent with a build-up of charge on the migrating oxygen at the transition state structure that accentuates its desire to participate in hydrogen bonding, a desire that is less in the reactant (similar effects were observed in other systems; see Table S1 in the Supporting Information for details). When two solvent molecules hydrogen bond to the oxygen of the methoxy substituent (**L**), the energy decreases by 5−7 kcal/mol compared to the case with only one methanol interacting with the methoxy group (**G**). In system **M**, in which both the migrating oxygen and the methoxy oxygen are doubly hydrogen bonded, the resultant energy barrier is actually slightly higher than that of **K**. This is again most likely due to interactions of the solvent molecules in the starting material; unlike the solvent molecules in reactant **K**, some methanol molecules in **M** hydrogen bond with each other rather that with the solute (in fact, the large barrier for **M**, as compared to that for **N**, is due in part to the fact that a hydrogen bonding interaction between two methanol molecules in the reactant, which is not present for system **N**, is lost as the reaction proceeds; see Table S1, Supporting Information). Model **N** contains solvent molecules at the four positions that each individually resulted in a decrease in the rearrangement barrier (see **E**, **F**, **G**, and **J**; Figure 6). The combination of all of these interactions leads to a barrier of only approximately 25 kcal/mol, suggesting that the effects of these interactions are nearly additive. The largest model we examined, **O**, contains six methanol molecules. In addition to the five solvent molecules present in **N**, it includes a methanol that was shown in **I** to cause a slight increase in the barrier (in terms of enthalpy). As seen in Figure 8, the additional methanol molecule (highlighted in box) orients itself in the transition-state structure for dyotropic rearrangement so as to participate in multiple interactions. Its alcohol proton interacts weakly (based on distances) with both the nitrogen and oxygen of the five-membered heterocycle, while its oxygen participates in a C−H···O interaction with the electron-deficient C−H bond on the migrating carbon.[13] While the C−H···O interaction would be expected to stabilize the buildup of positive charge and help the rearrangement, the interactions with the nitrogen and oxygen atoms are expected to hinder rearrangement (see **H** and **I**, Figure 6). Consequently, the barrier for rearrangement of **O** is somewhat larger than that for **N** due to these unfavorable interactions. Note also that, as a result of these interactions, this transition-state structure is significantly looser (i.e., more dissociative, especially with regard to the migrating oxygen) than that for **D** (Figure 5).

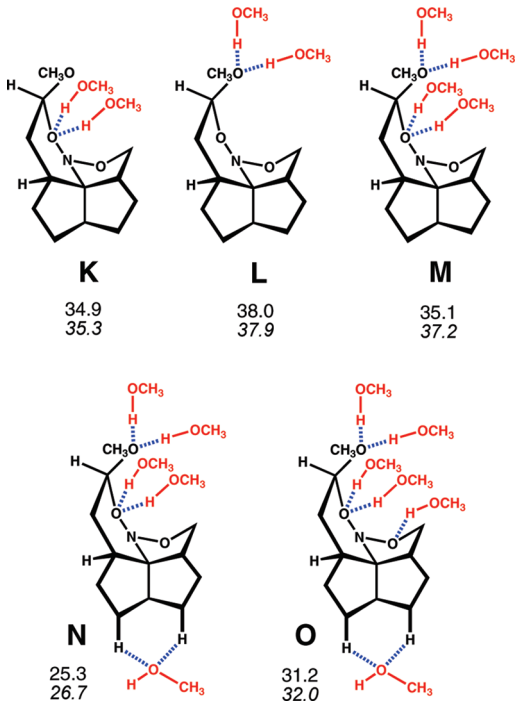

FIGURE 7. Computed barriers (B3LYP/6-31G(d); kcal/mol) for dyotropic rearrangements of models **K**−**O**. All energies are reported in kcal/mol and are relative to the energy of the starting material (ZPE-corrected energies in normal text; free energies at room temperature in italics).

Does the combination of the specific and nonspecific solvation effects discussed above lower the rearrangement barrier to an experimentally relevant value? We do not expect these two effects to be simply additive, since the solvent continuum will screen the effects of intramolecular electrostatic interactions to some extent. To determine the combined effects, the energy barrier for **O** was recalculated in a methanol continuum.[14] The resulting barrier was 24 kcal/mol,[15] 7 kcal/mol less than that for **O** (Figure 7), more than 10 kcal/mol less than that for **D** in a solvent continuum (vide supra), and nearly 25 kcal/mol less than that for the gas-phase rearrangement of **D** (Figure 5). Thus, when both specific and nonspecific solvation effects are accounted for, along with structural effects, the inherent barrier for dyotropic rearrangement of the sort observed for **1** (nearly 70 kcal/mol based on model **A**, Figure 1) is reduced by more than 40 kcal/mol, down to an experimentally relevant value.[15]

Explicit Protonation. Given that the rearrangement of **1** was reported to occur in a weakly acidic environment (SiO_2, EtOAc), the effects of explicit protonation on the reaction were also explored. The rearrangement of model system **P** (Figure 9; a protonated version of **D**) was examined.[16]

(14) Due to the size and complexity associated with the large number of solvent molecules, only single-point energy calculations in solvent were run on the fully optimized gas-phase starting material and transition-state structure for model **O**.

(15) When these calculations were repeated using a larger basis set (6-31+G(d,p)), the energy barrier was lowered by another 2 kcal/mol.

(16) Proton transfer to **D** was also modeled using SiH_3OH as a model proton donor. Protonation of the migrating oxygen is accompanied by cleavage of the N−O bond and has a barrier of 27 kcal/mol in the gas phase (24 kcal/mol in a methanol continuum). This model neglects to account for intramolecular hydrogen bonds that occur in silica and for solvent interactions with the silica, which also affect the acidity of silica, however, and likely overestimates the barrier for proton transfer.

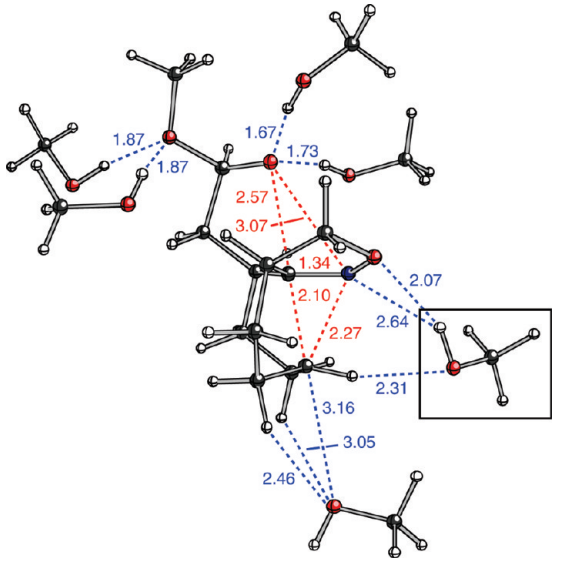

FIGURE 8. Transition-state structure for rearrangement of **O** (rotated compared to views of transition-state structures shown in previous figures). Selected distances are given in Å.

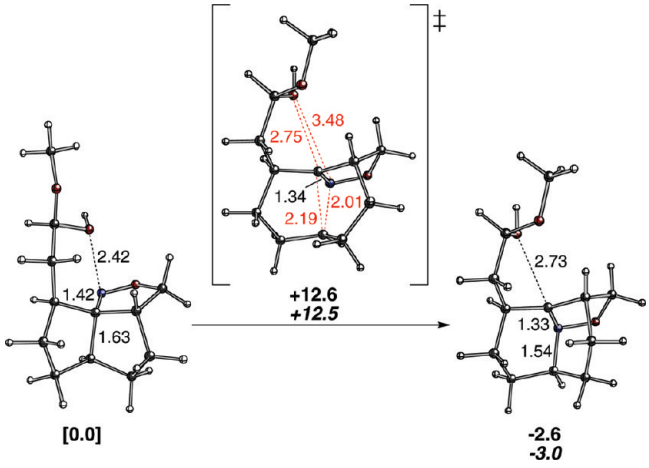

FIGURE 9. B3LYP/6-31G(d)-optimized geometries of reactant, transition-state structure, and product for the rearrangement of **P**. All energies are reported in kcal/mol and are relative to the energy of the reactant (ZPE-corrected energies in normal text; free energies at room temperature in italics). Selected bond lengths are given in Å.

Optimization of the protonated reactant results in cleavage of the $N-O_{migrating}$ bond. The rearrangement can still proceed from this structure though, with **P** undergoing a 1,2-alkyl shift (e.g., Figure 9; this is also possible for other conformers of the protonated reactant; see the Supporting Information) followed by ring closure upon deprotonation. Although the 1,2-shift has a lower barrier than concerted dyotropic rearrangement in nonprotonated systems, explicit protonation is not essential for rearrangement, as described above.[17]

Other Nitroso Acetals. Having determined the roles of structure and solvent in promoting the rearrangement of **1**, we next examined the **3**-to-**4** rearrangement (Scheme 2) using an analogous approach. The most important structures are

(17) Note that no products of trapping of intermediates from the rearrangement of **P** were reported.

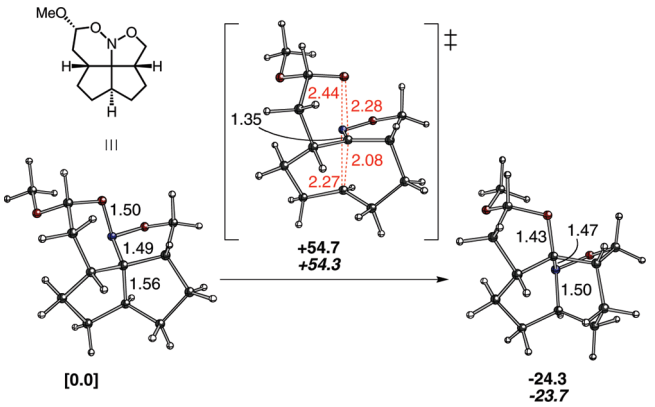

FIGURE 10. B3LYP/6-31G(d)-optimized geometries of reactant, transition-state structure, and product for the rearrangement of **Q**. All energies are reported in kcal/mol and are relative to the energy of the reactant (ZPE-corrected energies in normal text; free energies at room temperature in italics). Bond lengths are given in Å.

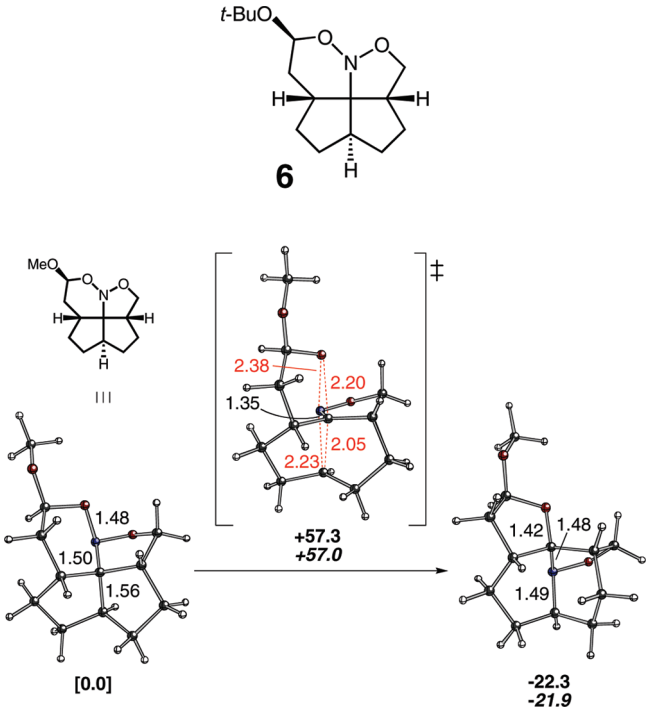

FIGURE 11. B3LYP/6-31G(d)-optimized geometries of reactant, transition-state structure, and product for the rearrangement of **R**. All energies are reported in kcal/mol and are relative to the energy of the reactant (ZPE-corrected energies in normal text; free energies at room temperature in italics). Bond lengths are given in Å.

discussed here, and details on smaller model systems can be found in the Supporting Information. Model system **Q**, a diastereomer of model system **D**, is shown in Figure 10. The gas-phase activation energy for the concerted dyotropic rearrangement of **Q** was found to be 54−55 kcal/mol. When explicit and implicit solvent interactions were accounted for (in analogy to model **O**) the barrier decreased to 29 kcal/mol. On the basis of these calculations, the rearrangement of **3** appears to be slightly less favorable than that of **1**, which may seem surprising given that O−N−C−C dihedral angle in **D** is 134°, while in **Q** it is 169°. However, the differential strain between the reactant

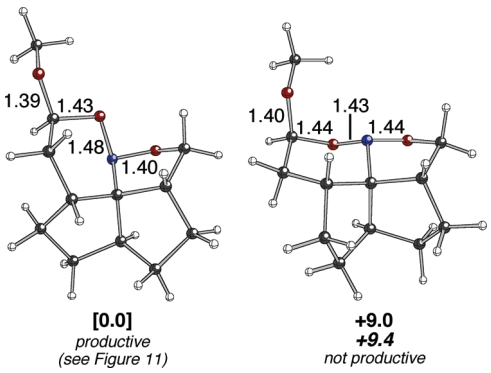

FIGURE 12. B3LYP/6-31G(d)-optimized geometries of the two chair conformations of **R**. All energies are reported in kcal/mol and are relative to the energy of the starting material (ZPE-corrected energies in normal text; free energies at room temperature in italics). Bond lengths are given in Å.

and transition-state structure for the rearrangement of **Q** appears to be greater than that for **D**; note that **D** starts out with a boatlike conformation for the ring bearing the methoxy group, and some of the eclipsing associated with this arrangement is relieved as the reaction proceeds.[18,19]

The final system examined, **6**, was designed by the Denmark group in an effort to construct a system that would not undergo dyotropic rearrangement so readily.[3] The hypothesis was that in such a system a nonproductive conformer would contain an axial alkoxy group that would now enjoy anomeric stabilization, lowering its energy relative to the productive conformer(s). Compound **6** did appear to be more resistant to dyotropic rearrangement, only undergoing partial rearrangement when exposed to silica.[3] This system was modeled using **R** (Figure 11). The productive conformer of **R** (Figure 11 and Figure 12, left) was actually found to be 9 kcal/mol lower in energy than the nonproductive conformer (Figure 12, right); while the anomeric stabilization associated with the alkoxy group is lost as expected for the productive conformer, lone pair$_O$ ↔ σ^*_{N-O} anomeric stabilization is lost for the nonproductive conformer. Nonetheless, the barrier for the dyotropic rearrangement was indeed predicted to be slightly higher for **R** in the gas phase than for **D** or **P**, although the predicted barrier was the same as for **P** (29 kcal/mol) when explicit and implicit solvent interactions were accounted for.[20]

Conclusions

Using density functional calculations, we examined dyotropic rearrangements of nitroso acetal-containing fennestranes that convert them to complex polycyclic aminals.[3] We predict these rearrangements should be extremely rapid if protonation of the reactant can occur but can also

(18) There is another productive conformer of reactant **Q** that is 0.6 kcal/mol lower in energy. In this structure (see the Supporting Information), the 6-membered ring adopts a twist-boat conformation, which is also (mostly) free of eclipsing interactions present in **D**. The transition-state structure for dyotropic rearrangement of this conformer is higher in energy (in both the gas phase and with explicit and implicit solvent) than that for the conformer shown in Figure 9.

(19) In **Q**, a chair-flip can occur for the ring bearing the alkoxy substituent that would lead to a conformer that is not productive for the dyotropic rearrangement. This alternative conformer is approximately 4 kcal/mol higher in energy than the productive conformers[18] (due at least in part to loss of the anomeric stabilization associated with an axial alkoxy group), and the conformational change is associated with low barriers. See the Supporting Information for details.

proceed without explicit protonation in a polar protic environment as a result of a fortuitous combination of structural and environmental effects. These effects, discussed herein in the context of a particular type of dyotropic rearrangement (one in which oxygen and carbon atoms migrate across a carbon−nitrogen unit), are also likely to be applicable to the various other types of dyotropic rearrangements receiving attention from the synthetic and mechanistic organic chemistry communities,[2] and we hope that the approach applied herein for unveiling the roles of particular structural and environmental effects will be useful in facilitating the rational design of additional synthetically useful dyotropic rearrangements.

(20) This system was also reexamined using a *tert*-butyl group in place of the methyl group (a *tert*-butyl group was present in the experimental system[3]), but the barrier for the dyotropic rearrangement changed by only 0.1 kcal/mol. See the Supporting Information for details.

Acknowledgment. We gratefully acknowledge the University of California−Davis, the National Science Foundation's Alliance for Graduate Education and the Professoriate program at UC Davis, the National Science Foundation's CAREER program (CHE-0449845), and the National Science Foundation's Partnership for Advanced Computational Infrastructure (CHE-030089, Pittsburgh Supercomputer Center) for support. We are particularly grateful to Scott Denmark (University of Illinois) for helpful suggestions.

Supporting Information Available: Coordinates and energies for all computed structures, additional information on computations not discussed in detail in the text, results of IRC calculations, and full GAUSSIAN citation. This material is available free of charge via the Internet at http://pubs.acs.org.